Fano effect and electronic correlations in double quantum dots: Aharonov–Bohm effect

2006 J. Phys.: Condens. Matter 18 1655

(http://iopscience.iop.org/0953-8984/18/5/018)

INSTITUTE OF PHYSICS PUBLISHING JOURNAL OF PHYSICS: CONDENSED MATTER

J. Phys.: Condens. Matter **18** (2006) 1655–1665 doi:10.1088/0953-8984/18/5/018

Fano effect and electronic correlations in double quantum dots: Aharonov–Bohm effect

Zhi-Yong Zhang

Department of Physics, Nanjing University, Nanjing 210093, People's Republic of China

Received 26 July 2005, in final form 20 September 2005
Published 18 January 2006
Online at stacks.iop.org/JPhysCM/18/1655

Abstract

The interplay between the Fano effect and electronic correlations in a double-quantum-dot (DQD) structure is investigated by the finite-U slave-boson mean-field method, and the focus is put on the influence of the Aharonov–Bohm (AB) effect on the transport properties. In the singly occupied regime, with weak antiferromagnetic correlation, the Fano–Kondo effect greatly suppresses the conductance G, whereas the strong parity splitting blocks the path through the DQD, which is similar to the time-reversal symmetric case. At the particle–hole symmetric point the peak usually still exists in the would-be peak-zero structure, but with the magnetic flux increased the zero is enhanced and eventually removed at quarter of a flux quantum. Results similar to the frequency doubling of AB oscillation and the 'pinning' of the AB maximum can be found, which account for the appearance of a new transmission zero in the variation of G with the energy levels on dots.

1. Introduction

The interplay between quantum interference and electronic correlations is important in mesoscopic physics. When a discrete energy level is embedded in a continuum energy state, the quantum interference between two configurations—one through the resonant level and the other directly through the continuum—leads to the Fano effect [1], a ubiquitous phenomenon first found in atomic physics then in other areas [2–5], which is characterized by an asymmetric line shape. Because of their tunability, quantum dot (QD) systems have attracted a lot of attention. When a dot is connected to leads, the coupling between the localized spin on the dot and conduction electrons leads to the Kondo correlation, which is described by an energy scale T_K, the so called Kondo temperature. When a dot is in the Kondo regime [6–10], a spin singlet state is formed by the localized spin and conduction electrons. This singlet state yields the Abrikosov–Suhl resonance and plays an important role in the electronic transport. When the Fano effect is introduced in a system with one QD, the so-called Fano–Kondo effect is found [2, 3, 11–14]. The recent development in nanofabrication techniques makes it possible to observe the Fano effect in electronic transport through a hybrid system of one QD and an

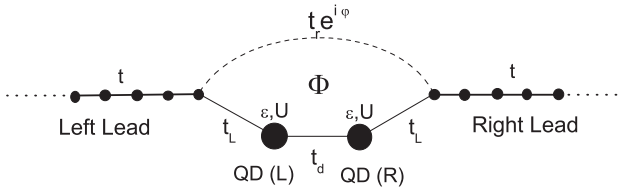

Figure 1. Schematic illustration of the DQD structure.

Aharonov–Bohm (AB) ring [4, 5], so that the relative phase between the two configurations can be artificially adjusted by an external magnetic flux Φ. The influence of the AB effect is studied on a QD system with the Fano coupling, and the frequency doubling of AB oscillation and the 'pinning' of the AB maximum are predicted in theory [11].

If double quantum dots (DQDs) [15–19] are coupled with each other by the tunnelling matrix element t_d, the Coulomb interaction U in dots yields an effective antiferromagnetic (AF) coupling $J_M = \sqrt{(2t_d)^2 + (U/2)^2} - U/2$ (or $\sim 4t_d^2/U$ if $t_d \ll U$). This coupling tends to create a singlet state between the localized spins on the two dots. When the two dots are connected to the left and right leads in a 'lead–dot–dot–lead' series, the competition between the Kondo and AF correlations yields a resonant conductance peak in $J_M \sim T_K$ at the particle–hole symmetric point [17–19], whereas in the limit $J_M \ll T_K$ and $t_d \gg U/4$ the conductance G approaches zero. In a recent paper [20], we have studied how the interplay between the Fano effect and electronic correlations affects the transport properties when the Fano effect is introduced in a DQD system. We find in the singly occupied regime, when $J_M \ll T_K$, the Fano–Kondo effect greatly suppresses G, whereas the strong parity splitting results in the blockade of the path through the DQDs. At the particle–hole symmetric point, the competition between the Kondo and AF correlations still leads to a resonant peak in $J_M \sim T_K$, but due to the Fano effect, the resonant peak is always accompanied with a transmission zero. This peak-zero structure governs the variation trend of G with the energy levels on dots.

However, in that work, the time-reversal symmetry is supposed and no external magnetic field is applied. Consequently, it is natural to ask, if an external magnetic flux Φ is applied, (i) how does G behave in the limits $J_M \to 0$ and ∞, (ii) how does the peak-zero structure change, and (iii) can the frequency doubling of AB oscillation and the 'pinning' of the AB maximum be found in DQD systems? To answer these questions, we assume a structure similar to that in [20], where two dots and two leads are arranged in a 'lead–dot–dot–lead' series and the two leads are also directly connected to each other (cf the schematic illustration of the structure in figure 1). But here, a magnetic flux Φ penetrates the area enclosed by the two paths. The finite-U slave-boson mean-field theory (f-U SBMFT) of Kotliar and Ruckenstein (KR) [19, 21, 22] is adopted to treat the electronic correlations. In the singly occupied regime, with $J_M \ll T_K$, the Fano–Kondo effect greatly suppresses the conductance, and with $t_d \gg U/4$ the strong parity splitting blockades the path through the DQDs. These results are similar to the situation with $\Phi = 0$. At the particle–hole symmetric point, in the would-be peak-zero structure around $J_M \sim T_K$, the peak usually still exists, but with Φ increased the zero is enhanced and eventually removed at quarter of a flux quantum. Phenomena similar to the frequency doubling of AB oscillation and the 'pinning' of the AB maximum can be found, which accounts for the appearance of a new transmission zero in the variation of G with the energy levels on dots.

The organization of this paper is as follows. In section 2, the theoretical model and calculation method are illustrated. In section 3, the numerical results and discussion of them are presented. A brief summary is given in section 4.

2. Model and formulae

In the present paper, we investigate the influence of an external magnetic flux on the transport properties through a DQD system at zero temperature under the interplay between the Fano effect and electronic correlations. In figure 1, the system is schematically illustrated, where two identical dots and two identical leads are arranged in a 'lead–dot–dot–lead' series and the two leads are also directly coupled to each other. Here, the two dots are taken as Anderson impurities, each of which has one single-particle energy level ϵ and an on-site Coulomb interaction U. The tunnelling matrix elements of dot–dot, dot–lead and lead–lead are $t_{\rm d}$, $t_{\rm L}$ and $t_{\rm r}$, respectively. As we know from [20], although the considered system is symmetric, the obtained results are robust to the detuning between the two dots only if the detuning is not too strong. But unlike [20], the time-reversal symmetry is broken by a magnetic flux Φ, which penetrates the area enclosed by the two paths. Because the two dots and their nearest neighbouring sites on leads can be regarded as forming an AB ring, and because no magnetic field is directly applied on the structure, we can make a convenient choice of the gauge for the vector potential to affect only the phase of the wavefunction at the direct hopping bond between the two leads [23], and Φ enters only the tunnelling matrix element of lead–lead $t_{\rm r}{\rm e}^{{\rm i}\varphi}$, where $\varphi = 2\pi\Phi/\Phi_0$, with $\Phi_0 = hc/e$ the flux quantum. Then, this mesoscopic system can be described by the following 1D tight-binding Hamiltonian:

$$H = H_{\rm L} + H_{\rm D} + H_{\rm T}, \tag{1}$$

where $H_{\rm L}$, $H_{\rm D}$ and $H_{\rm T}$ are the Hamiltonians of leads, dots and the coupling between dots and leads. They are

$$H_{\rm L} = -t\left[\sum_{i=-\infty,\sigma}^{-2} + \sum_{i=1,\sigma}^{\infty}\right](c_{i\sigma}^{\dagger}c_{i+1\sigma} + {\rm H.c.}), \tag{2}$$

$$H_{\rm D} = \sum_{\alpha=L,R}\left(\sum_{\sigma}\epsilon c_{\alpha\sigma}^{\dagger}c_{\alpha\sigma} + Un_{\alpha\uparrow}n_{\alpha\downarrow}\right) - t_{\rm d}\sum_{\sigma}(c_{L\sigma}^{\dagger}c_{R\sigma} + {\rm H.c.}) \tag{3}$$

and

$$H_{\rm T} = -\sum_{\sigma}(t_{\rm L}c_{-1\sigma}^{\dagger}c_{L\sigma} + t_{\rm L}c_{1\sigma}^{\dagger}c_{R\sigma} + t_{\rm r}{\rm e}^{{\rm i}\varphi}c_{1\sigma}^{\dagger}c_{-1\sigma} + {\rm H.c.}), \tag{4}$$

with the spin index $\sigma = \uparrow$ or $\downarrow$.

If one dot with energy level ϵ and Coulomb repulsion U is connected to leads with the hopping integral $t_{\rm L}$, the Kondo temperature can be expressed as [24] $T_{\rm K} = \frac{U\sqrt{J_{\rm K}}}{2\pi}\exp(-\pi/J_{\rm K})$, with $J_{\rm K} = \frac{-2U\Gamma}{\epsilon(\epsilon+U)}$. Here, the hybridization strength $\Gamma = \pi\rho(\epsilon_{\rm F})t_{\rm L}^2$, with $\rho(\epsilon_{\rm F})$ the density of states at the Fermi energy. The correlation length of a spin singlet at zero temperature $\xi_{\rm K} = \hbar v_{\rm F}/T_{\rm K}$, with $v_{\rm F}$ the Fermi velocity. In the thermodynamic limit [25], $\Gamma = 2t_{\rm L}^2/t$ and $\xi_{\rm K} = 2t/T_{\rm K}$ at $\epsilon_{\rm F} = 0$. In the present paper, we always set $\epsilon_{\rm F} = 0$. On the other hand, in the DQD system, if $t_{\rm L}$ is set as zero, electrons can only tunnel through the direct channel. At this time, the transmissivity is $|T_{\rm r}|^2 = \frac{4}{(t_{\rm r}/t+t/t_{\rm r})^2}$.

The f-U SBMFT of KR [19, 21] is adopted to treat the electronic correlations. It is a powerful nonperturbative tool to study the strongly correlated fermion system, and is not limited to the infinite-U case [26]. In the DQD structure, the AF coupling J_M is introduced implicitly by this method as a function of U and $t_{\rm d}$, but not as an artificial parameter in the Hamiltonian [16]. In the framework of this approach, eight auxiliary boson fields e_α, $p_{\alpha\sigma}$ and d_α are introduced, which act as projection operators onto the empty, singly occupied and doubly occupied electronic states at the dot 'α', respectively. To eliminate the unphysical states, six

constraints are imposed: $\sum_\sigma p^\dagger_{\alpha\sigma}p_{\alpha\sigma} + e^\dagger_\alpha e_\alpha + d^\dagger_\alpha d_\alpha = 1$ and $c^\dagger_{\alpha\sigma}c_{\alpha\sigma} = p^\dagger_{\alpha\sigma}p_{\alpha\sigma} + d^\dagger_\alpha d_\alpha$. To obtain exact results in the noninteracting limit, the fermion operator $c_{\alpha\sigma}$ should be replaced by $c_{\alpha\sigma}z_{\alpha\sigma}$, with $z_{\alpha\sigma} = (1 - d^\dagger_\alpha d_\alpha - p^\dagger_{\alpha\sigma}p_{\alpha\sigma})^{-1/2}(e^\dagger_\alpha p_{\alpha\sigma} + p^\dagger_{\alpha\bar{\sigma}}d_\alpha)(1 - e^\dagger_\alpha e_\alpha - p^\dagger_{\alpha\bar{\sigma}}p_{\alpha\bar{\sigma}})^{-1/2}$. Therefore, the Hamiltonian (1) can be replaced by the following effective Hamiltonian:

$$H_{\rm eff} = H_{\rm L} + \tilde{H}_{\rm D} + \tilde{H}_{\rm T} + \sum_{\alpha=L,R}\left\{\lambda^{(1)}_\alpha\left(\sum_\sigma p^\dagger_{\alpha\sigma}p_{\alpha\sigma} + e^\dagger_\alpha e_\alpha + d^\dagger_\alpha d_\alpha - 1\right)\right.$$
$$\left. + \sum_\sigma \lambda^{(2)}_{\alpha\sigma}(c^\dagger_{\alpha\sigma}c_{\alpha\sigma} - p^\dagger_{\alpha\sigma}p_{\alpha\sigma} - d^\dagger_\alpha d_\alpha)\right\}, \tag{5}$$

where the six constraints are incorporated by the six Lagrange multipliers $\lambda^{(1)}_\alpha$ and $\lambda^{(2)}_{\alpha\sigma}$. The original $H_{\rm D}$ and $H_{\rm T}$ are changed to

$$\tilde{H}_{\rm D} = \sum_{\alpha=L,R}\left(\epsilon\sum_\sigma c^\dagger_{\alpha\sigma}c_{\alpha\sigma} + U d^\dagger_\alpha d_\alpha\right) - t_{\rm d}\sum_\sigma(z^\dagger_{L\sigma}c^\dagger_{L\sigma}c_{R\sigma}z_{R\sigma} + {\rm H.c.}) \tag{6}$$

and

$$\tilde{H}_{\rm T} = -\sum_\sigma\left(t_{\rm L}c^\dagger_{-1\sigma}c_{L\sigma}z_{L\sigma} + t_{\rm L}c^\dagger_{1\sigma}c_{R\sigma}z_{R\sigma} + t_{\rm r}{\rm e}^{{\rm i}\varphi}c^\dagger_{1\sigma}c_{-1\sigma} + {\rm H.c.}\right), \tag{7}$$

whereas $H_{\rm L}$ remains unchanged.

To solve the effective Hamiltonian (5), we can integrate out the fermionic variables from the corresponding effective action, write down the saddle-point free-energy functional, and then determine the expectation values of boson fields by minimization of the saddle-point free-energy functional at zero temperature as KR did in their original paper [21]. But, this approach is equivalent to a mean-field approximation in which the slave-boson fields are first replaced by their expectation values, then the values of e_α, $p_{\alpha\sigma}$, d_α, $\lambda^{(1)}_\alpha$ and $\lambda^{(2)}_{\alpha\sigma}$ are obtained by minimization of the ground state energy E_0 of the essentially noninteracting effective Hamiltonian (5) with respect to these parameters [22]. This leads to a set of self-consistent equations [19, 22]. Because of the spin degeneracy, only ten variational parameters should be determined. They are e_α, p_α, d_α, $\lambda^{(1)}_\alpha$, and $\lambda^{(2)}_\alpha$. To construct these self-consistent equations, we need knowledge of the ground state $|0\rangle$. It is obtained from the calculation of a cluster, at the centre of which is located the DQD structure. The single-particle eigenstates can be calculated by direct numerical diagonalization, and the ground state $|0\rangle$ is constructed by adding electrons to the lowest unoccupied levels one by one until the Fermi level. If the cluster size is much larger than $\xi_{\rm K}$, the results obtained from the cluster calculation can be regarded as those of the original system [27, 28].

As soon as these variational parameters are obtained, the conductance G through the structure at zero temperature can be obtained from the two-terminal Landauer–Büttiker (LB) formula:

$$G = |T(\epsilon_{\rm F})|^2, \tag{8}$$

because the effective Hamiltonian (5) is essentially noninteracting [29]. Here $T(\epsilon_{\rm F})$ is the transmission coefficient of an incident electron with the Fermi energy. In writing the above equation, the spin index and the unit $2e^2/h$ are omitted. For continuum models, some authors adopted the LB formula combined with the slave-boson mean-field method to calculate G via the Green function technique [13, 19]. But for a tight-binding Hamiltonian, the transmission coefficient T can be calculated more straightforwardly via the transfer matrix (TM) method [30, 31]. The transfer matrixes corresponding to the effective noninteracting Hamiltonian (5) hold the same forms as those corresponding to the original Hamiltonian (1)

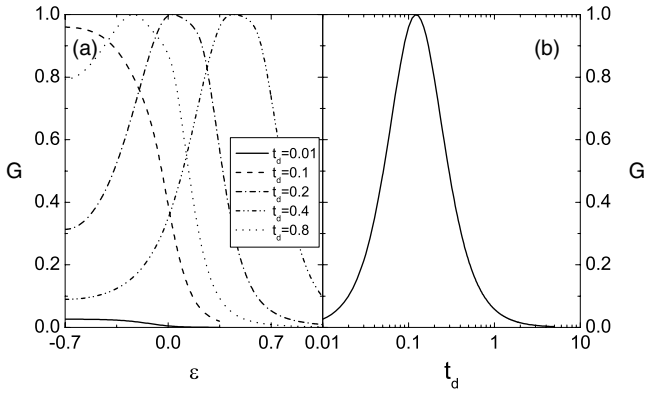

Figure 2. (a) G–ϵ curves with $t_{\rm d} = 0.01$ (solid), 0.1 (dashed), 0.2 (dotted), 0.4 (dash–dotted) and 0.8 (dash–dot–dotted) and (b) G–$t_{\rm d}$ curve with $\epsilon = -U/2$ for $t_{\rm r} = 0$. The other parameters are $t = 1$, $t_{\rm L} = 0.35$ and $U = 1.4$.

when the Coulomb interaction U is set as 0 in equation (1). In the mean-field approximation, the electron–electron interaction is represented in the transfer matrixes by the replacement of the undressed parameters by the renormalized ones: $\tilde{\epsilon}_\alpha = \epsilon + \lambda_\alpha^{(2)}$, $\tilde{t}_{\rm d} = t_{\rm d} z_{\rm L} z_R$ and $\tilde{t}_{L_\alpha} = t_{\rm L} z_\alpha$. This is similar to that in the conductance calculation via the Green function technique [13, 19].

3. Results and discussion

To compare the results with the previous work, we take the same parameters as in [20]. They are $t = 1$, $U = 1.4$ and $t_{\rm L} = 0.35$. Consequently, $T_{\rm K}$ and $\xi_{\rm K}$ are 0.0280 and 71.5, respectively, at the particle–hole symmetric point $\epsilon = -U/2$. To guarantee good convergence, the cluster size is set as 800 with $t_{\rm d} < 0.1$, 400 with $0.1 \leqslant t_{\rm d} < 0.2$ and 200 with $0.2 \leqslant t_{\rm d}$ in the determination of the variational parameters.

Although the results of the time-reversal symmetric case have been obtained in [20], they are briefly presented here for the convenience of readers. We first give our attention to the situation with $t_{\rm r} = 0$, which is illustrated in figure 2, and compare it with the exact numeric results. In figure 2(a), the G–ϵ curves with different $t_{\rm d}$ are given. Here and below, only the right parts with $\epsilon \geqslant -U/2$ are plotted, because the G–ϵ curves are symmetric with respect to $\epsilon = -U/2$. For $t_{\rm d} = 0.01$ and 0.1, a plateau is found in the singly occupied regime, and its height is close to unity with $t_{\rm d} = 0.1$ and close to zero with $t_{\rm d} = 0.01$. For $t_{\rm d} = 0.2$, 0.4 and 0.8, the plateau splits into two resonant peaks. With $t_{\rm d}$ increased, the splitting is strengthened and the G value at $\epsilon = -U/2$ is decreased. For any $t_{\rm d}$, in the empty and doubly occupied regimes, G always approaches zero. In figure 2(b), the G–$t_{\rm d}$ curve at $\epsilon = -U/2$ is given. With $t_{\rm d} \to 0$, $J_M \ll T_{\rm K}$ and two Kondo spin singlets are formed between the localized spins on dots and conduction electrons on the adjacent leads. Because the tunnelling between the two singlet states is very small, G approaches zero. When $t_{\rm d} \gg U/4$, the parity splitting leads to the double occupancy on the bonding orbital of the two dots, which tends to block the electronic transport. A resonant peak emerges at $t_{\rm d}^R = 0.12$, which corresponds to $J_M = 0.04 \sim T_{\rm K}$. This resonant peak characterizes the competition between the Kondo and AF correlations. Here, the values of J_M for a series of $t_{\rm d}$ are given in table 1. Comparing figures 2(a) and (b), we can see that only when $t_{\rm d} \geqslant t_{\rm d}^R$ can resonant peaks appear in the G–ϵ curves. All of these are consistent with the exact numeric results [17, 18], and, albeit a mean-field method, the f-U SBMFT grasps the basic physics of the DQD structure.

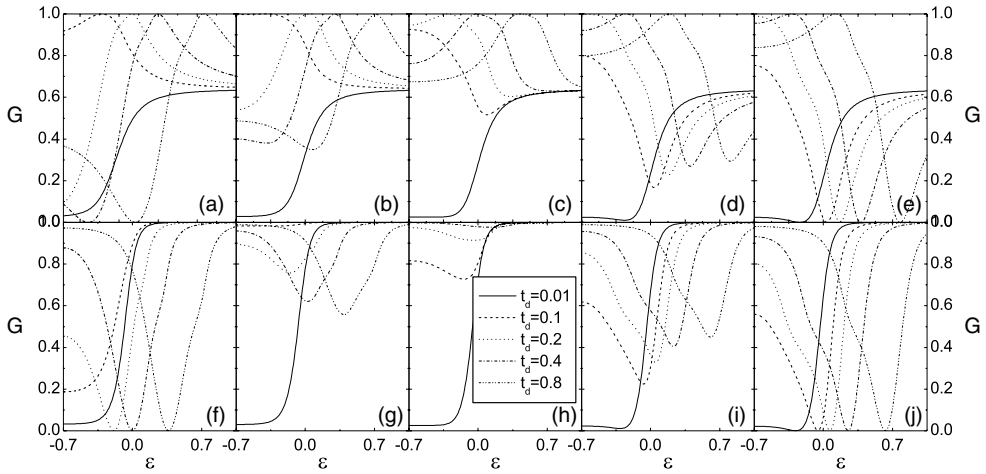

Figure 3. G–ϵ curves with $t_r = 0.5$ (upper row) and 1 (lower row). From the left column to the right, φ increases from 0 to π with an interval of $\pi/4$. Lines with different textures correspond to different t_d, with $t_d = 0.01$ (solid), 0.1 (dashed), 0.2 (dotted), 0.4 (dash–dotted) and 0.8 (dash–dot–dotted). The other parameters are the same as in figure 2.

Table 1. Table of $J_M = \sqrt{(2t_d)^2 + (U/2)^2} - U/2$ with $U = 1.4$. When $t_L = 0.35$, $T_K = 0.0280$, which is almost identical to the J_M at $t_d = 0.1$.

t_d	0.01	0.1	0.12	0.2	0.4	0.8
J_M	2.86×10^{-4}	0.0280	0.0400	0.106	0.363	1.05

In figures 3(a) and (f), we plot the G–ϵ curves for $\varphi = 0$ with $t_r = 0.5$ and 1, respectively. The direct tunnelling cannot eliminate the electronic correlations in the system, but introduces the quantum interference between different channels. As in the system with a single QD [11, 12], G always approaches $|T_r|^2$ when $|\epsilon + U/2| \gg 0$. (Here, $|T_r|^2 = 0.64$ for $t_r = 0.5$ and 1 for $t_r = 1$.) For $t_r = 0.5$, in the G–ϵ curves with $t_d = 0.4$ and 0.8 there are one resonant peak and one transmission zero, but with $t_d = 0.1$ and 0.2 only one resonant peak appears, and with $t_d = 0.01$ neither resonant peak nor transmission zero emerge. The same character is also found for $t_r = 1$, but here the resonant peaks are merged into the tails with unit conductance. As we have said, because the G–ϵ curves are symmetric for a DQD system, only the right parts with $\epsilon \geqslant -U/2$ are plotted. In fact, the resonant peak (transmission zero) appears in a pair. This is different from the system with a single QD, where one resonant peak and one transmission zero always appear simultaneously and are located at the opposite sides of the particle–hole symmetric point, which leads to asymmetric G–ϵ curves. The G–t_d curves at $\epsilon = -U/2$ for $t_r = 0.5$ and 1 are plotted in figures 4(a) and (b), respectively, by solid lines. For any t_r, G approaches zero if t_d is close to zero. This is a clear demonstration of the Fano–Kondo effect: if $t_d = 0$, the two dots are decoupled from each other and can be regarded as side-coupled to a 1D chain. The electrons tunnelling through one side-coupled QD structure can take two different paths—one through the energy level on the dot and the other directly through the continuum, which leads to an exact zero conductance in the Kondo regime [13]. Consequently, no matter whether t_r is strong or weak, the conductance of the whole system is exactly zero. When t_d is introduced, the Kondo correlation still dominates and that kind of Fano–Kondo effect plays a major role if $J_M \ll T_K$. This explains the appearance

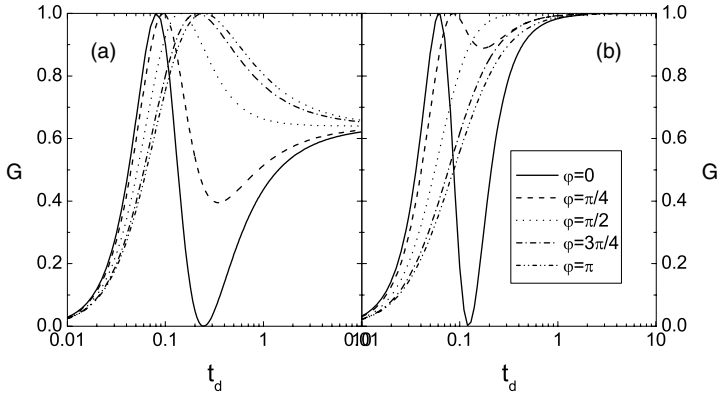

Figure 4. G–t_d curves with $\epsilon = -0.7$ and $U = 1.4$ for $t_r = 0.5$ (a) and 1 (b). Lines with different texture correspond to different φ, with $\varphi = 0$ (solid), $\pi/4$ (dashed), $\pi/2$ (dotted), $3\pi/4$ (dash–dotted) and π (dash–dot–dotted).

of the low plateau in the singly occupied regime with $t_d = 0.01$ in figures 3(a) and (f). With $J_M \sim T_K$, the competition between the Kondo and AF correlations still yields a resonant peak in G–t_d curves. But the introduction of quantum interference between the direct channel and the path through the two dots leads to a transmission zero accompanied with the resonant peak. This is a demonstration of the interplay between the Fano effect and the competition of the Kondo and AF correlations. If the positions of peak and zero are set as t_d^R and t_d^D, respectively, only when $t_d > t_d^{R(D)}$ can the resonant peak (transmission zero) appear in the G–ϵ curves. In the G–t_d curves, with t_d further increased, G approaches $|T_r|^2$, the transmissivity through the direct channel. In this regime, the strong parity splitting leads to double occupancy on the bonding orbital. This results in the blockade of the channel through the DQDs, and the quantum interference disappears.

All of the above results have been obtained in our previous work [20] (where the qualitative relations between t_d^R (t_d^D) and t_r have also been obtained, but they are not given here). Now, we turn our attention to the situation with $\varphi \neq 0$. Because of the phase locking property of the two-terminal conductance $G(\varphi) = G(-\varphi)$, only the results with $\varphi \in [0, \pi]$ are given. The variation of G with ϵ is presented in figure 3, where curves with identical φ and different t_d are illustrated in the same graph. Graphs in the upper row correspond to structures with $t_r = 0.5$ and those in the lower one to $t_r = 1$. As in the situation with $\varphi = 0$ [20], G always approaches $|T_r|^2$ when $|\epsilon + U/2| \gg 0$. When $t_d = 0.01$, a low plateau is formed in the singly occupied regime for any t_r and φ. As we have said in the preceding paragraph, for $\varphi = 0$, the appearance of a low plateau in the singly occupied regime with $t_d = 0.01$ is the consequence of the Fano–Kondo effect. Now, we can see that with $J_M \ll T_K$ the influence of the AB effect is weak in that regime. This is another difference between the DQD system and the single QD one, where the Fano–Kondo effect is characterized by a suppressed Kondo plateau for $\varphi = 0$, and the plateau height is sensitive to the external magnetic flux. This difference is entirely caused by the different structures of the two systems. In the single-QD system the dot is embedded in the arm parallel to the direct channel, whereas in the DQD system the two dots are side-coupled to leads at $t_d = 0$. When $t_d \neq 0$ but $J_M \ll T_K$, the Kondo correlation prevails over the AF one, and in the Kondo regime the two dots can be first regarded as side-coupled to leads. Although the Fano effect plays an important role in both of these two systems, the different interference configurations lead to the different properties of the Fano–Kondo effect.

These characteristics are similar to those of the time-reversal symmetric case. However, breaking the time-reversal symmetry also introduces some new characteristics. Under a specific set of t_d and t_r, with φ introduced, the resonant peak in a G–ϵ curve, if it appears when $\varphi = 0$, is usually kept with the same t_d and t_r. But its position is moved towards the negative ϵ direction, and because of this movement it is possible for a would-be resonant peak to disappear. Meanwhile, with φ increased from zero, the transmission zero is enhanced, and at $\varphi = \pi/2$, quarter of a flux quantum, the corresponding residual dip almost entirely disappears. However, with φ further increased a new dip emerges, which is located farther away from the particle–hole symmetric point than the remaining resonant peak, and when $\varphi = \pi$, half of a flux quantum, a new transmission zero is formed for every t_d, even $t_d = 0.01$. But as illustrated in figures 3(a) and (f), for $\varphi = 0$, neither resonant peak nor transmission zero can be found for $t_d = 0.01$. This new emerging transmission zero is caused by the AB effect. These results can be found for both $t_r = 0.5$ and 1, and the only difference between these two situations is that the resonant peak for $t_r = 1$ is merged into the tail with unit conductance.

In figures 4(a) and (b), the influence of φ on the G–t_d curves is illustrated for structures with $t_r = 0.5$ and 1, respectively. According to our experience on the situation with $\varphi = 0$, we hope that the G–t_d curve at the particle–hole symmetric point can also govern the variation trend of G with ϵ when $\varphi \neq 0$. For any φ, G approaches zero with $t_d \to 0$ because of the Fano–Kondo effect [13], which is consistent with the appearance of a low conductance plateau in the singly occupied regime. In the other limit with $t_d \gg U/4$, the strong parity splitting leads to the double occupancy on the bonding orbital, which blockades the channel through the DQDs, and G approaches $|T_r|^2$. These properties are identical with the time-reversal symmetric case. In the intermediate region, the quantum interference between two paths—one through the direct channel and the other through the two dots via t_d—plays an important role. With $\varphi = 0$, the competition between the Kondo and AF correlations leads to a resonant peak, which is accompanied by a transmission zero coming from the quantum interference destruction. As an external magnetic flux is applied, the relative phase of electronic wave functions through different paths is changed, and the condition of quantum interference destruction is no longer satisfied. The zero in the peak-zero structure is enhanced, and when $\varphi = \pi/2$ the corresponding residual dip is removed entirely. As a result, the peak is merged into the tail with unit conductance for $t_r = 1$, whereas for $t_r = 0.5$, or more generally for $t_r \neq 0$ and 1, the peak always exists, but its position is moved towards positive direction. At $\varphi = \pi$, although it looks a little like the line shape of the G–t_d curve with $t_r = 0$, the preserved peak does not come purely from the competition between the Kondo and AF correlation, but from the interplay between the quantum interference and the electronic correlations. (Of course, with $t_d \gg U/4$, G approaches different values for t_r being and not being zero.) It is the AB effect that turns the would-be peak-zero structure into a peak. These results are consistent with the movement of resonant peaks in G–ϵ curves and can account for the removal of transmission zeros at $\varphi = \pi/2$. However, for $\varphi > \pi/2$, the peak-zero structure in G–t_d curve is destroyed by the AB effect and the zero disappears. Where does the new transmission zero in the G–ϵ curve come from?

In figure 5, the variation of G with ϵ is presented in a different manner, where curves with identical t_d and different φ are illustrated in the same graph. As in figure 3, the upper row of graphs corresponds to $t_r = 0.5$ and the lower to $t_r = 1$. Consider the situation with $t_r = 0.5$ first. In a structure with $t_d = 0.01$, as φ increases, a dip emerges in the mixed-valence regime, and at $\varphi = \pi$, this dip is turned into a transmission zero. At any specific ϵ, G decreases monotonically as φ is increased from zero to π. Because of the phase locking of the two-terminal conductance, only the results with $\epsilon \in [0, \pi]$ are given, and practically G oscillates with φ in a period of 2π. With $t_d = 0.1$, as φ increases, the resonant peak moves towards the

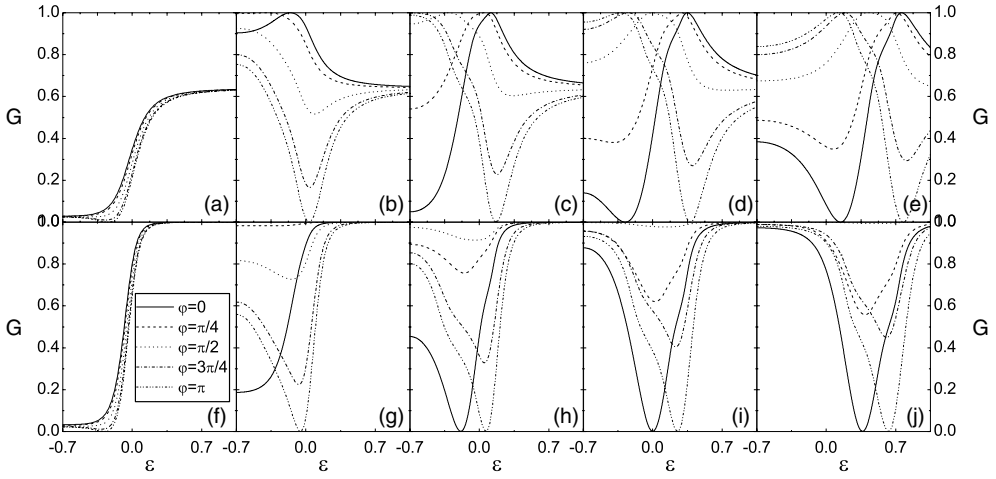

Figure 5. G–ϵ curves with $t_r = 0.5$ (upper row) and 1 (lower row). From the left column to the right, $t_d = 0.01$, 0.1, 0.2, 0.4 and 0.8, respectively. Lines with different textures correspond to different φ, with $\varphi = 0$ (solid), $\pi/4$ (dashed), $\pi/2$ (dotted), $3\pi/4$ (dash–dotted) and π (dash–dot–dotted). The other parameters are the same as in figure 2.

negative direction and disappears. Meanwhile, a dip emerges, which turns into a transmission zero at $\varphi = \pi$. Compared with that for $t_d = 0.01$, the position of this transmission zero moves towards the doubly occupied regime. Here, G also decreases monotonically with φ except in the range from $\epsilon = -U/2$ to about -0.24, where G first increases with φ then decreases and a component of period π enters the G oscillation. With $t_d = 0.2$, the nonmonotonic range is expanded and the position of the new emerging transmission zero is further moved. A variation trend of the G–ϵ curve similar to the 'pinning' of the AB maximum [11] is found in structures with $t_d = 0.4$ and 0.8. Compared with the G–ϵ curves in figure 2(a) for $t_r = 0$, the resonant peak is recovered when $\varphi = \pi/2$, and the G–ϵ curve for φ looks 'symmetric' with that for $\pi - \varphi$. But in a system with one QD, it is the resonant Kondo plateau that is recovered when $\varphi = \pi/2$. In a DQD system, the recovered resonant peak is out of the singly occupied regime. It is in the mixed-valence regime when $t_d = 0.4$, and is further moved with larger t_d. Despite this difference, the 'pinning' of the AB maximum found in these two types of systems results from the same origin—the AB effect. Similarly, the new emerging transmission zero in the G–ϵ curve for $\varphi = \pi$ also comes from the change of the relative phase between the two paths caused by the external magnetic flux. Meanwhile, with $t_d = 0.4$ and $0.8G$ monotonically increases and decreases with φ at $\epsilon = -U/2$ and $3U/4$, respectively, whereas in the intermediate region around the recovered resonant peak G first increases with φ then decreases, a phenomenon resembling the frequency doubling of the AB oscillation found in single-QD systems [11]. In the situation with $t_r = 1$, this phenomenon can also be found, but the variation of G is not strictly monotonic at $\epsilon = -U/2$ and $3U/4$ for $t_d = 0.4$ and 0.8, although the amplitude of variation is small.

Despite the fact that there is no structure in the G–t_d curve which is connected with the new emerging transmission zero in the G–ϵ curve, the properties given in the preceding paragraph are consistent with those exhibited in figure 4. For $t_r \neq 0$, at the particle–hole symmetric point, G monotonically decreases (increases) with φ in the range $0 \leqslant t_d < t_d^B$ ($t_d^U \leqslant t_d < \infty$). In the intermediate region, G first increases then decreases as φ is changed from zero to π. The 'pinning' of the AB maximum and the frequency doubling of AB oscillation can only happen

for $t_d > t_d^U$. For $t_r = 0.5t_d^B$ and t_d^U are 0.086 and 0.22, respectively, whereas for $t_r = 1$, because $|T_r|^2 = 1$, the peak in the G–t_d curve is merged into the tail with unit conductance when $\varphi \geqslant \pi/2$ and t_d^U approaches infinity. The situation with $t_r = 1$ can be regarded as an extreme case. Here, for simplicity of calculation, we only give the results of $t_r = 0.5$ as a representative for $t_r \neq 1$, but the basic properties exhibited in these results are irrelevant with the specific value of t_r.

4. Summary

In summary, we investigate the interplay between the Fano effect and electronic correlations in a DQD system by the f-U SBMFT, and pay attention to the influence of the AB effect on the transport properties through the structure. Despite the introduction of φ, in the singly occupied regime, with $J_M \ll T_K$, the Fano–Kondo effect greatly suppresses the conductance, whereas with $t_d \gg U/4$ the strong parity splitting blockades the path through the DQDs, which is similar to the time-reversal symmetric case. At the particle–hole symmetric point, in the would-be peak-zero structure resulting from the interplay between the Fano effect and the competition between the Kondo and AF correlations, the peak still exists, but with φ increased the zero is enhanced and eventually removed at $\varphi = \pi/2$, which corresponds to quarter of a flux quantum. Results similar to the frequency doubling of AB oscillation and the 'pinning' of the AB maximum can be found, which account for the appearance of a new transmission zero in the variation of G with the energy level ϵ on dots.

Acknowledgments

The author acknowledges support by the National Foundation of Natural Science in China grant No 10204012, and by the special funds for Major State Basic Research project No G001CB3095 of China.

References

[1] Fano U 1961 *Phys. Rev.* **124** 1866
[2] Göres J *et al* 2000 *Phys. Rev.* B **62** 2188
[3] Zacharia I G *et al* 2001 *Phys. Rev.* B **64** 155311
[4] Kobayashi K, Aikawa H, Katsumoto S and Iye Y 2002 *Phys. Rev. Lett.* **88** 256806
[5] Kobayashi K, Aikawa H, Katsumoto S and Iye Y 2003 *Phys. Rev.* B **68** 235304
[6] Goldhaber-Gordon D, Shtrikman H, Mahalu D, Abusch-Magder D, Meirev U and Kaster M A 1998 *Nature* **391** 156
[7] Cronewett S M, Oosterkamp T H and Kouwenhoven L P 1998 *Science* **281** 540
[8] Simmel F, Blick R H, Kotthaus U P, Wegsheider W and Blichler M 1999 *Phys. Rev. Lett.* **83** 804
[9] van der Wiel W G, De Franceschi S, Fujisawa T, Elzerman J M, Tarucha S and Kouwenhoven L P 2000 *Science* **289** 2105
[10] Ji Y, Heiblum M, Sprinzak D, Mahalu D and Shtrikman H 2000 *Science* **290** 779
[11] Hofstetter W, König J and Shoeller H 2001 *Phys. Rev. Lett.* **87** 156803
[12] Bulka B R and Stefanski P 2001 *Phys. Rev. Lett.* **86** 5128
[13] Kang K, Cho S Y, Kim J J and Shin S C 2001 *Phys. Rev.* B **63** 113304
[14] Franco R, Figueira M S and Anda E V 2003 *Phys. Rev.* B **67** 155301
[15] Aono T, Eto M and Kawamura K 1998 *J. Phys. Soc. Japan* **67** 1860
[16] Georges A and Meir Y 1999 *Phys. Rev. Lett.* **82** 3508
[17] Büsser C A, Anda E V, Lima A L, Davidovich M A and Chiappe G 2000 *Phys. Rev.* B **62** 9907
[18] Izumida W and Sakai O 2000 *Phys. Rev.* B **62** 10260
[19] Dong B and Lei X L 2002 *Phys. Rev.* B **65** 241304
[20] Zhang Z-Y 2005 *J. Phys.: Condens. Matter* **17** 1617

[21] Kotliar G and Ruckenstein A E 1986 *Phys. Rev. Lett.* **57** 1362
[22] Dorin V and Schlottmann P 1993 *Phys. Rev.* B **47** 5095
[23] Byers N and Yang C N 1961 *Phys. Rev. Lett.* **7** 46
[24] Hewson A C 1993 *The Kondo Problem to Heavy Fermions* (Cambridge: Cambridge University Press)
[25] Kang K and Shin S-C 2000 *Phys. Rev. Lett.* **85** 5619
[26] Coleman P 1984 *Phys. Rev.* B **29** 3035
[27] Affleck I and Simon P 2001 *Phys. Rev. Lett.* **86** 2854
[28] Hu H, Zhang G-M and Yu L 2001 *Phys. Rev. Lett.* **86** 5558
[29] Meir Y and Wingreen N S 1992 *Phys. Rev. Lett.* **68** 2512
[30] Simon P and Affleck I 2003 *Phys. Rev.* B **68** 115304
[31] Xiong S J and Evangelou S N 1995 *Phys. Rev.* B **52** 13079